AGU PUBLICATIONS

Geophysical Research Letters

RESEARCH LETTER
10.1002/2016GL068547

Key Points:
- Hydrogen flux inferred from water-rock interaction matches Earth observations
- Modeled Europa hydrogen flux from water-rock interaction is similar to Earth's
- Inferred high Europa oxidant flux suggests similar redox as in the Earth system

Supporting Information:
- Supporting Information S1
- Figure S1

Correspondence to:
S. D. Vance,
svance@jpl.nasa.gov

Citation:
Vance, S. D., K. P. Hand, and R. T. Pappalardo (2016), Geophysical controls of chemical disequilibria in Europa, *Geophys. Res. Lett.*, *43*, 4871–4879, doi:10.1002/2016GL068547.

Received 7 MAR 2016
Accepted 29 APR 2016
Accepted article online 17 MAY 2016
Published online 24 MAY 2016
Corrected 13 JUL 2016

This article was corrected on 13 JUL 2016. See the end of the full text for details.

Geophysical controls of chemical disequilibria in Europa

S. D. Vance[1], K. P. Hand[1], and R. T. Pappalardo[1]

[1] Jet Propulsion Laboratory, California Institute of Technology, Pasadena, California, USA

Abstract The ocean in Jupiter's moon Europa may have redox balance similar to Earth's. On Earth, low-temperature hydration of crustal olivine produces substantial hydrogen, comparable to any potential flux from volcanic activity. Here we compare hydrogen and oxygen production rates of the Earth system with fluxes to Europa's ocean. Even without volcanic hydrothermal activity, water-rock alteration in Europa causes hydrogen fluxes 10 times smaller than Earth's. Europa's ocean may have become reducing for a brief epoch, for example, after a thermal-orbital resonance ~2 Gyr after accretion. Estimated oxidant flux to Europa's ocean is comparable to estimated hydrogen fluxes. Europa's ice delivers oxidants to its ocean at the upper end of these estimates if its ice is geologically active, as evidence of geologic activity and subduction implies.

1. Introduction

In potentially habitable worlds, global fluxes of oxygen and hydrogen provide a measure of chemical disequilibria, a key requirement for life. Pressure and temperature control geochemical production of these redox couples. They also control the presence of oceans in oceanic icy worlds: the Galilean satellites Europa, Callisto [*Khurana et al.*, 1998], and Ganymede [*Kivelson et al.*, 2002]; and in Saturn's moons Enceladus [*Postberg et al.*, 2009; *Iess et al.*, 2014] and Titan [*Bills and Nimmo*, 2005; *Iess et al.*, 2012]; and probably Neptune's moon Triton [*Chyba et al.*, 1989; *Nimmo and Spencer*, 2014]. Today, each of these worlds may contain the ingredients for life—the fluxes of chemical energy, water, and raw materials that make up cellular material and drive biogeochemistry. Possible past ocean worlds in the solar system, with extinct or remnant subsurface oceans, include the asteroid Ceres [*McCord and Sotin*, 2005; *Castillo-Rogez and McCord*, 2010; *Castillo-Rogez*, 2011]; icy satellites Ariel, Iapetus, Umbriel, Titania, Oberon, and Triton; and large dwarf planets including Pluto, Charon, Eris, Sedna, and Orcus [*Hussmann et al.*, 2006; *Vance et al.*, 2007; *Rhoden et al.*, 2015].

Pressures and temperatures common to the water-rock interfaces in known and putative ocean-bearing icy worlds, past and present, are outside the "terrestrial planet habitable zone" range in which life grows on Earth (Figure 1). High hydrostatic pressures (approaching 2000 MPa) [*Vance et al.*, 2014] and depression of fluid freezing points by compounds such as ammonia must be considered when addressing life's adaptability [*Rothschild and Mancinelli*, 2001; *Picard and Daniel*, 2013]. In Europa and Enceladus, Earth-like seafloor pressures of <100 MPa and modest temperature conditions [*Hsu et al.*, 2015] make them prime candidates in the search for extant life. We argue that these conditions also imply a high degree of water-rock reaction today, even in the absence of tidal heating in the mantle.

Here we consider how internal pressures and temperatures in wet and rocky worlds govern hydrogen production from water-rock reactions. As described in section 2, we compute the *P-T* conditions for thermal cracking (thick line in Figure 1), as a conservative metric for the limits to water percolation into the rocky mantle. Water-rock interaction rates are computed for material exposed as the fracture front moves downward due to global cooling. Serpentinization has been shown to produce hydrogen at low temperatures [*Mayhew et al.*, 2013] and so is used as a basis for our estimates of hydrogen fluxes, allowing comparison with production estimates for Earth obtained from in situ measurements. In section 3 we discuss the results and implications for Europa: Europa likely has a high radiolytic oxidant flux and comparable low-temperature and high-temperature sources of reductants. We consider how Europa may have changed through time, and whether Europa's global ocean system has a long-lived redox cycle comparable to the Earth system.

2. Reductants From Low-Temperature Water-Rock Reactions

Today, Earth's low-temperature water-rock alteration and high-temperature hydrothermalism produce comparable fluxes of hydrogen [*Sleep and Bird*, 2007]. Water-rock reactions to more than 5 km depth in Earth's

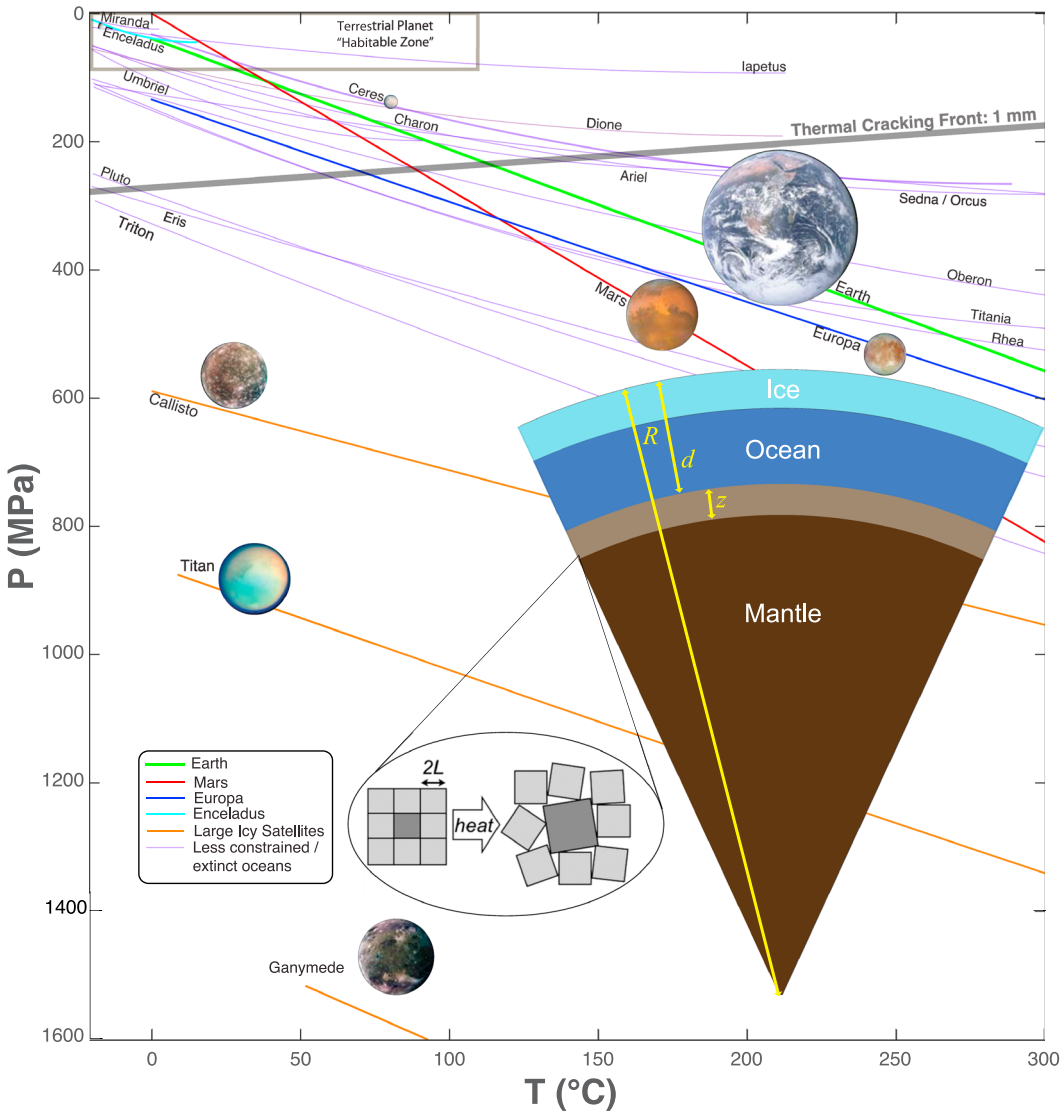

Figure 1. Pressures and temperature profiles for known and putative ocean worlds used in the fracture model. The inset schematic, modified from *Neveu et al.* [2015], illustrates the mechanism for cracking due to thermal expansion anisotropy.

oceanic and continental crust produce abiogenic hydrogen in abundances exceeding 2×10^{11} mol yr^{-1} [*Sherwood Lollar et al.*, 2007, 2014]. Serpentinization contributes the majority of Earth's reaction-derived H_2, releasing both heat and hydrogen from hydration of olivine and pyroxene [*Sleep et al.*, 2004]:

$$3Fe_2SiO_4 + 2H_2O = 2Fe_3O_4 + 3SiO_2(aq) + 2H_2(aq) \quad (1)$$

fayalite + water = magnetite + silica + hydrogen

$$3FeSiO_3 + H_2O = Fe_3O_4 + 3SiO_2(aq) + H_2(aq) \quad (2)$$

ferrosilite + water = magnetite + silica + hydrogen.

$$2Mg_2SiO_4 + 3H_2O = Mg(OH)_2 + Mg_3Si_2O_5(OH)_4 \quad (3)$$

forsterite + water = brucite + serpentine.

Serpentinization has occurred throughout the solar system, as evidenced in ancient regions on Mars [*Michalski et al.*, 2013] and in carbonaceous chondrites [*Takir et al.*, 2013] that are representative of early solar system materials. These findings support the idea that deep low-temperature water-rock reactions contribute to the

global redox inventory on Europa (or Mars), contrary to prior assumptions [*Jakosky and Shock*, 1998; *Travis et al.*, 2012; *Pasek and Greenberg*, 2012].

We calculate global hydrogen production rates using the fracture model from *Vance et al.* [2007]. Symbols are described in Table S1 in the supporting information and planetary values in Table S2. Fracturing exposes unaltered rock progressively through time. For a planet or moon with radius R and seafloor depth d ($R_{sf} = R - d$) as shown in Figure 1, the mass of fresh rock exposed per unit time, $\dot{M}$, and associated heat H_{serp} and hydrogen production F_{H_2} from serpentinization of olivine are computed from the advancing depth $z(t)$ ($R_h(t) = R_{sf} - z(t)$) of the fracture front below the seafloor,

$$V(t) = 4/3\pi(R_{sf}^3 - R_h(t)^3) \tag{4}$$

$$\dot{n_{fo}} = \dot{V}/V_{fo} \tag{5}$$

$$H_{serp} = x_{ol} L_{serp} \dot{n_{fo}} \tag{6}$$

$$F_{H_2} = \frac{2}{3} x_{ol} x_{fa} \dot{n_{fo}}. \tag{7}$$

The exposure of reactable rock $\dot{n}_{fo}$ (in moles) assumes the specific volume of the major component forsterite (V_{fo} = 43.79 cm^3 mol^{-1}). We adopt the forsterite reaction heat, which is known at standard pressures and temperatures of serpentinization (L_{serp} = 41 kJ mol^{-1}) [*MacDonald and Fyfe*, 1985; *Früh-Green et al.*, 2004]. Oxidizing a mole of fayalite with water generates 2/3 of a mole of hydrogen (equation (3)). We thus assume 10^3 mol m^{-3} of reacted rock, less than the value of 1.4×10^3 mol m^{-3} assumed by *Sherwood Lollar et al.* [2014]. We ignore additional production of hydrogen from radiogenic hydrolysis of water [*Lin et al.*, 2005].

The compositional structure of Europa's mantle is uncertain and depends in part on the vigor of mantle convection during its early history (see Text S2). Rock composition is assumed to be that of lherzolite, the most common peridotite in Earth's mantle, with 70% olivine (x_{ol} = 0.7), 10% of which is iron-bearing fayalite (x_{fa} = 0.1). The remaining 30% is not consequential to our model, but is worth describing in further detail (see supporting information Text S3).

We compute $z(t)$ as the pressure and temperature horizon below which the fracture opening rate exceeds the rate of viscous closure. Microfracturing is caused by thermal expansion anisotropy and mismatch (inset schematic in Figure 1), which are linked to cooling. This creates openings, or flaws, between mineral grains, creating porosity, which equates with permeability on the ~Myr time scales considered here.

The depth of fracturing depends on grain and flaw sizes (assumed as 1 and 0.1 μm, respectively) and cooling rate (1 °C yr^{-1}). The grain size is a conservative lower limit; grain sizes in planetary seafloors are probably larger, which would lead to higher fluxes of hydrogen (see supporting information for further discussion and details). Fracturing depends most strongly on grain size; on smaller worlds, mineral grain sizes will be larger in general (see supporting information) and thus will be more susceptible to fracturing. We assume rock rheological and thermal properties consistent with olivine in Earth's crust.

The fracture front deepens as global radiogenic heating decreases. Unaltered rock is exposed at rates, $\dot{z}$, on the order of millimeter per year (Table S2). We compute time-dependent pressure-temperature profiles in icy worlds from known bulk densities and assessed internal radiogenic heating. We assume the bodies are differentiated into a pure water upper layer with an underlying rocky core (Figures 1 and supporting information) [*Vance et al.*, 2007]. Constraints on internal density distributions are presently unavailable for many objects (magenta in Figure 1). We do not account for the effects of high pressures and dense ice phases on the chemistry of water-rock interactions in the largest icy worlds (orange in Figure 1) (pressure for Ganymede is computed using depth dependent gravity and thermodynamic properties as in *Vance et al.* [2014]).

Our model assumes exposed olivine serpentinizes immediately, but we implicitly adopt a relevant time scale >1 Myr, appropriate for near-complete fracturing of exposed olivine.

The thermal fracturing model provides conservative estimates of fluid-accessible depths in icy worlds. The model does not include factors that could create additional permeability [*Sleep*, 2012]. These include large-scale tectonism, which on Earth subsumes water into the oceanic crust [*McCaig*, 1988], and additional cracking from fluid overburden pressure or expansion/contraction within pores, as discussed by *Neveu et al.* [2015] in the elaboration of this model and its application to Ceres. We ignore dissolution and precipitation

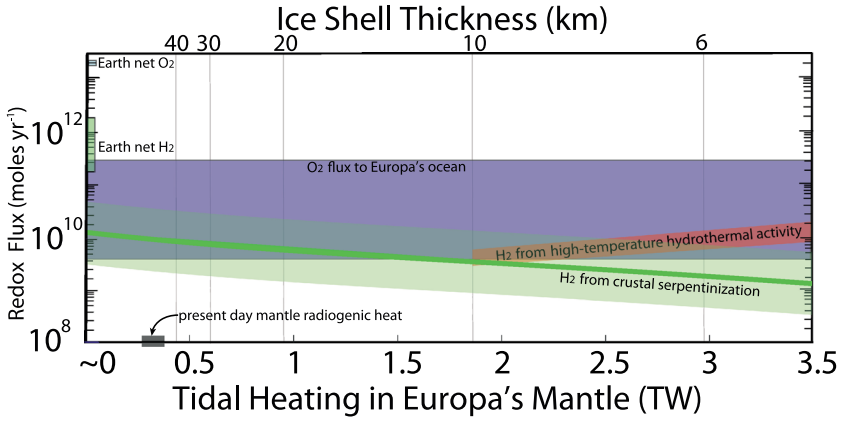

Figure 2. Present-day fluxes of H_2 and O_2 to Europa's ocean versus tidal heating in the rocky interior. Top axis: equilibrium thickness of a thermally conductive ice shell heated from below.

of materials, which may enhance or reduce permeability (*Neveu et al.* [2015] find effects from dissolution and precipitation of magnesium carbonate, chrysotile serpentinite, and silica to be negligible). Volume increase due to serpentinization, another possible inhibitor of porosity, in fact appears to aid in the formation of additional fractures [*O'Hanley*, 1992; *Kelemen and Hirth*, 2012]. Permeability measurements in multiple rock types indicate precipitated products of serpentinization decrease permeability by up to 2 orders of magnitude [*Farough et al.*, 2016]. However, neutron diffraction studies of partially serpentinized rocks [*Tutolo et al.*, 2016] suggest that permeability increases in long-lived flow channels due to flow or diffusion within pores, partially offsetting the volume increase upon serpentinization by precipitation of denser magnetite, and due to the development of porosity within the serpentinites themselves.

3. Results

By this method, predicted hydrogen flux for Earth is similar to values assumed and measured by others. The depth of water-rock reaction is $z = 6$ km, similar to "habitable zone" depths of 5 km assumed by *Sherwood Lollar et al.* [2014] and *Sleep and Bird* [2007]. Seismic measurements constrain hydrothermal circulation depths to <10 km [*deMartin et al.*, 2007]. This depth limit is also inferred for the West Canadian shield from geothermal, thermochronological, and (U-Th)/He dating measurements. The predicted rate of material exposure in Earth's present-day crust, $\dot{z} = 0.03\mu m\ yr^{-1}$, is 100 times less than the $2.5\mu m\ yr^{-1}$ inferred by *Flowers et al.* [2006]. We attribute the difference to our assumption that objects cool uniformly over 4.5 Gyr, whereas the West Canadian shield was emplaced within the past 1.7 Ga. Hydrogen production from serpentinization, integrated over Earth's entire surface, is 2×10^8 mol $cm^{-2}\ s^{-1}$ or 0.5×10^{11} mol $H_2\ yr^{-1}$. This is similar to inventories from hydration of continental Precambrian crust in the range $0.2–1.8 \times 10^{11}$ mol $H_2\ yr^{-1}$ [*Sherwood Lollar et al.*, 2014].

Water-rock alteration should occur more extensively in objects smaller than Earth because fracturing depths scale inversely with an object's radius (supporting information Table 2). Enceladus is expected to fracture throughout its rocky interior at the time of accretion, neglecting any tidal heating. If the fracturing model is correct, the high hydrogen and methane concentrations observed in the Enceladus plumes [*Waite et al.*, 2009], and high inferred ocean pH consistent with active serpentinization [*Glein et al.*, 2015], would imply the ocean is relatively young, perhaps owing to recent migration into tidal resonance with Dione, or alternatively that serpentinization has proceeded very slowly.

Europa's predicted present-day hydrogen production (Figure 2) is nearly an order of magnitude larger than Earth's on a per-unit-area basis (Figure 3). Rock exposure rate ($\dot{z}$ in Table S2) is 0.1 $\mu m\ yr^{-1}$. Predicted fracture depth for a present-day 100 km deep ocean is 25 km. Europa produces up to 4×10^{10} mol of H_2 per year from water-rock reactions with newly exposed material. In the largest icy bodies—Titan, Ganymede, and Callisto—and in bodies with a very thick H_2O upper layer such as Triton, high pressures prevent microfracture formation, so water-rock reactions in these objects require additional mechanisms to generate permeability, such as tectonics, pore fluid expansion, or fluid overburden.

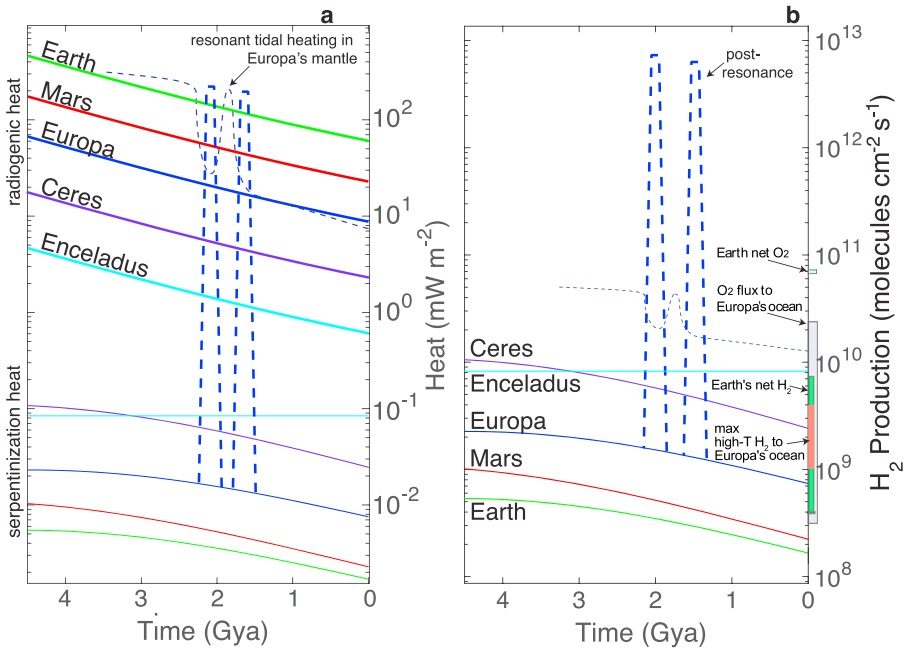

Figure 3. (a) Heat (in mW m^{-2}) and (b) hydrogen (in molecules cm^{-2} s^{-1}) from serpentinization in wet and rocky worlds versus geologic time (in Gya). Dashed lines: reequilibration of the alteration front due to a resonance of Europa's thermal and orbital evolution [*Hussmann and Spohn*, 2004]. Shaded regions in Figure 3b at 0 Gya: H_2 and O_2 fluxes to Europa's ocean and Earth's atmosphere from Figure 2.

3.1. Hydrogen From High-Temperature Hydrothermalism

Europa's reductant flux may be maintained by serpentinization or high-temperature (~350°C) basaltic volcanism. High-temperature hydrothermal fluids on Earth have a global mass flux $Q_{ht} \approx 3 \times 10^{13}$ kg yr^{-1} and produce $F_{H_2} \approx 0.06$ Tmol H_2 yr^{-1} [*Sleep and Bird*, 2007]. Earth's total flux of hydrothermal fluids is $Q_{hydr} = 10^{15}$ to $> 10^{17}$ kg yr^{-1} [*Johnson and Pruis*, 2003; *Nielsen et al.*, 2006]. *Lowell and DuBose* [2005] compute Europa's maximum global hydrothermal fluid mass flux to be $Q_{hydr} = 10^7$ kg s^{-1} or $\sim 3 \times 10^{14}$ kg yr^{-1}. They assume $H_{hydr} = 0.5H_{mantle} = 5$ TW, with H_{mantle} accounting for the majority of Europa's tidal heating. This extreme is unlikely today. The mantle is probably too viscous to dissipate significant tidal heat [*Sotin et al.*, 2009], although it was probably warmer and less viscous, and thus more dissipative early in Europa's history, as discussed below. The proportion of high-temperature fluid fluxes is assumed to be larger than on Earth, $H_{ht} = 0.1$ to $0.5H_{hydr}$, given Europa's lower gravity and steeper thermal gradient in the tidally heated mantle.

We calculate Europa's high-temperature hydrothermal H_2 production by analogy to Earth, based on global fluid fluxes. High-temperature hydrothermal hydrogen fluxes as a function of H_{mantle} are calculated as $F_{H_2,ht} = n_{H_2} Q_{ht}$, with $H_{ht} = 0.1H_{hydr} = 0.05H_{mantle}$. High-temperature mass flux is

$$Q_{ht} = \frac{H_{ht}}{c_w \Delta T}, \tag{8}$$

where $\Delta T = 350^o$C and $c_w = 4$ kJ kg^{-1} is the heat capacity of water at 350°C and Europan seafloor pressures in the range 100 MPa [*Wagner and Pruss*, 2002]. Nominal hydrogen content is $n_{H_2} = 2$ to 6 mmol H_2 kg^{-1} [*Holland*, 2002]. Applying this to the maximum H_{mantle} from *Lowell and DuBose* [2005] sets an upper bound for high-temperature hydrothermal reductant flux of ~0.03 Tmol H_2 yr^{-1}, comparable to the amount for Earth. Figure 2 shows $F_{H_2,ht}$, as a function of mantle tidal heating, up to $H_{mantle} = 3.5$ TW.

3.2. Oxidants: Magnetic Fields and Radiolysis

Among known icy worlds, oxidant production is largest at Europa because of its active geology and intense surface irradiation [*Cooper et al.*, 2001; *Johnson*, 2004; *Hand et al.*, 2007]. Gas giant magnetospheres capture solar wind ions that bombard satellite surfaces. Europa, Ganymede, and Callisto receive averages of 125, 6, and 0.6 mW m^{-2} [*Cooper et al.*, 2001; *Johnson*, 2004]. Enceladus and Triton receive less flux than Ganymede [*Cooper et al.*, 2009].

Surface irradiation dissociates water and drives radiation chemistry that oxidizes the surface to a depth greater than 10 cm [*Hand et al.*, 2007]. Oxygen-rich materials (O_2, H_2O_2, SO_4, SO_2, CO_2,...) accumulated at Europa's surface may reach its ocean on a time scale shorter than the nominal surface age of 60–100 Myr [*Zahnle et al.*, 2008] or longer if they are retained within the ice.

Estimates of present-day oxygen flux to Europa's ocean vary based on assumptions of how the surface ice overturns, with values ranging from 3×10^8 to 2×10^{11} mol O_2 yr^{-1} [*Hand et al.*, 2007] to as high as 1 to 3×10^{11} [*Greenberg*, 2010]. The higher values stem from assumptions that ridge and chaos formation bring fresh ice to Europa's surface, and melting within the ice aids in carrying materials to the ocean. The net effect is that resurfacing over time has cycled the oxidized upper layer back into the ice. In this scenario, continuous resurfacing would have enhanced the radiation gardening depth by a factor of 100 and saturated downwelling ice with oxidants over the first ~2 Gy of Europa's history.

Recent research supports the idea that Europa's ice is currently cycling surface materials into the ice and ocean. Subsumption [*Kattenhorn and Prockter*, 2014] and mobile subsurface liquids [*Schmidt et al.*, 2011] are tentatively identified in the few well imaged regions of Europa that may represent its global geology. If Europa's active ice shell delivers oxygen to the ocean at rates close to the upper bound of 3×10^{11} mol O_2 yr^{-1} [*Greenberg*, 2010], this is within 2 orders of magnitude of Earth's net photosynthetic oxygen flux of 2×10^{13} mol O_2 yr^{-1} [*Catling and Claire*, 2005].

3.3. Mind the Gap: The Redox Budget of the Europa System

Figure 2 shows Europa's present-day redox inventory compared with Earth's. Fluxes to Europa's ocean of H_2 from serpentinization or volcanism (10^9 to 5×10^{10} mol yr^{-1}) are in nearly the same range as those from O_2 from radiolysis (5×10^9 to 4×10^{11} mol yr^{-1}) with serpentinization compensating for the shutoff of volcanism in the case of low tidal heat input to Europa's rocky interior. The maximum seafloor heat (surface equivalent flux of 114 mW m^{-2}) [*Vance and Goodman*, 2009] represents the limit that Europa's ice is thinner than 6 km (top axis) and all tidal heating occurs in the rocky interior. As described above, this extreme is unlikely today, and the majority of tidal heat probably dissipates instead in Europa's ice [*Sotin et al.*, 2009]. We calculate thermally conductive ice thicknesses as per *Vance et al.* [2014], with T_s=110 K and T_b = 273 K. The thick line for H_2 flux corresponds to a rocky seafloor 100 km below Europa's surface; the shaded region surrounding it portrays uncertainties based on interpretation of *Galileo* gravity data (80-170 km) [*Schubert et al.*, 2004]). The width of the red line corresponds to high temperature H_2 in the range of 2 to 6 mmol kg^{-1} [*Holland*, 2002].

3.4. The Europa System Through Time

We can speculate on how the redox state of Europa's ocean has changed through time, and how this might have affected the evolution of a potential biosphere. The order of magnitude excess of present-day new O_2 fluxes over H_2 in Europa is comparable to Earth's present-day excess. On a per-unit-area basis, the absolute fluxes are also similar within an order of magnitude. It is worth considering whether gradual oxidation of Europa's ocean from an initially reducing state could have set the stage for a global biosphere mediated by cycling of carbon, nitrogen, and sulfur [*Hand et al.*, 2009; *Greenberg*, 2010].

A promising scenario for life's origin on Earth is a transition from geochemistry to biochemistry occurring in alkaline hydrothermal systems, in a mildly acidic ocean created by high-temperature volcanic and hydrothermal activity [*Russell et al.*, 2014, and references therein]. The first metabolic activity would have arisen from reduction of oceanic CO_2 using hydrogen from ~100 °C serpentinization, combined with abiotic methane from higher temperature water-rock reactions. Europa's early ocean and seafloor were probably also reducing, such that an independent origin of life might have occurred in the hot early Europa as its ocean oxidized by radiolysis [*Zolotov and Kargel*, 2009].

Metazoans, i.e., multicellular life, may have evolved if Europa's ocean oxidized in a manner similar to the gradual rise of oxygen in Earth's atmosphere [*von Strandmann et al.*, 2015; *Zhang et al.*, 2016]. Alternatively [*Greenberg*, 2010; *Pasek and Greenberg*, 2012], the oxidation of Europa's ocean could have overwhelmed reductive sinks at Europa's seafloor after the first ~2 Gyr, making the ocean toxic for life as we know it. *Pasek and Greenberg* [2012] assume that seafloor alteration was inadequate to buffer against toxic ocean acidification because mineral dissolution and incomplete hydration would have halted the progressive serpentinization described here (and summarized by *Vance and Goodman* [2009]). As noted earlier, the fracturing assumed

in our model is conservative relative to other estimates of fracture-induced permeability [*Sleep*, 2012; *Neveu et al.*, 2015]. Recent investigations of hydrogen flux on Earth [*Sherwood Lollar et al.*, 2014] support our model's predicted degree of water-rock alteration.

In contrast with the toxic acidification scenario, Europa's entire ocean may have become highly reducing for epochs lasting for millions of years, if its coupled thermal-orbital evolution led to intense heating in its silicate mantle. Though tidal heating of Europa's silicate mantle may be negligible today compared with radiogenic heating [*Sotin et al.*, 2009], it could have been larger during Europa's first few billion years due to higher orbital eccentricity and a warmer mantle. Europa's mantle may have received significant tidal heating during the 500 My after formation owing to a peak in thermal-orbital evolution of its Laplace resonance with Io. In models by *Hussmann and Spohn* [2004] in which the majority of tidal heat is generated in the silicate interior, this resulted in near-zero thickness of the conductive thermal layer in the rocky seafloor, with average temperatures in the convecting mantle exceeding the equilibrium hydration line for olivine and pyroxene (650 K; Figure S1). This type of dewatering is a key factor in plate subduction and volcanism on Earth [*Fyfe*, 1985]. Subduction also delivers oxidized iron (Fe^{3+}) from the crust to the lower mantle, restoring the reducing power of the crust [*Hayes and Waldbauer*, 2006].

If dehydration and subduction returned Europa's seafloor rocks to a reduced state by restoring Fe^{3+} to Fe^{2+}, rehydration in the subsequent epochs of cooling could have created spikes in the output of heat and hydrogen. These spikes are depicted as thin dashed lines in both panes of Figure 3, using tidal heating and crustal thickness numbers adopted from *Hussmann and Spohn* [2004, Figure 5]. The upper limit of corresponding heat and hydrogen fluxes (assuming the dehydrated mantle becomes fully reduced once more) is calculated as before, assuming mantle minerals become hydrated to the radiogenic fracture front depth z within 100 Myr. In that case, reductant output would have exceeded the present-day global flux of oxidants by orders of magnitude.

4. Discussion and Conclusions

Europa and other wet and rocky worlds may produce reductant fluxes comparable to Earth's on a per-unit-area basis (Figure 3). Europa is special for the potential to have a high flux of oxidants to its ocean. We predict that Europa's large and persistent chemical fluxes of oxygen and hydrogen, approximately 10^{11} and 10^{10} mol yr^{-1} today, respectively, could balance in a way that is unique among potentially habitable icy worlds in the solar system. For this reason, Europa may have favored the origin and evolution of life.

Earth's redox cycle is far more complex than the balance of hydrogen and oxygen fluxes we have discussed. The offset between Earth's O_2 and H_2 (Figures 2 and 3) reflects the role of carbon and to a lesser extent sulfur, iron, nitrogen, and other compounds. As described above, cycling of reductants and oxidants on Europa [*Hand et al.*, 2009; *Russell et al.*, 2014] may involve alteration of Europa's mantle by solid-state convection.

Several researchers have previously considered whether abundant abiotic oxidants on Europa could have prompted the evolution of metazoans [*Greenberg*, 2010; *Pasek and Greenberg*, 2012; *Hand et al.*, 2009, ibid.]; however, it has also been argued that complex life requires Earth-like continents to provide necessary minerals and diverse chemical reactions [e.g., *Maruyama et al.*, 2013]. The presence of potassium rich KREEP, granites, and other minerals has not been thoroughly evaluated for Europa. If such materials are required, it seems plausible that mantle solid-state convection might have provided sufficient heat to drive metamorphic separation of such "continental" materials, but this is speculative at the moment. Further work is needed, on Earth and at Europa, to determine the conditions for evolving complex life [e.g., *Lane and Martin*, 2010; *Pittis and Gabaldón*, 2016], and whether Europa may have produced such conditions.

Future missions can test the assumptions of our model by sampling Europa's atmosphere and ice for compositional and isotopic signatures of ocean pH and water-rock interaction [e.g., *Glein et al.*, 2015]. Gravity science [*Pauer et al.*, 2010; *Vance et al.*, 2015] or a landed seismic investigation [e.g., *Pappalardo et al.*, 2013] can aid in evaluating Europa's radial density structure, the rheological state and thermal state of its mantle [*Cammarano et al.*, 2006; *Panning et al.*, 2006], and the extent of seafloor hydration.

Acknowledgments
S.D.V. conceived of the work, performed the analysis, and wrote the manuscript. K.P.H. helped with development of the initial concept, writing of the initial manuscript, and subsequent refinement. R.T.P. helped with finalizing the work. This work benefitted immensely from discussions with Bruce Bills, J. Michael Brown, Mark Claire, Chris Glein, Matthew Pasek, Michael Russell, Christophe Sotin, and Kevin Zahnle. We thank the editor and two anonymous reviewers for thorough and helpful comments. This work was partially supported by NASA Outer Planets Research grants NNH12ZDA001N, by the Icy Worlds node of NASA's Astrobiology Institute (08-NAI5-0021 and 13-13NAI7_2-0024), and by the Europa Project. The research was carried out at the Jet Propulsion Laboratory, California Institute of Technology, under a contract with the National Aeronautics and Space Administration. All data for this paper are properly cited and referred to in the reference list. Matlab files for the calculations are available by request to S.D.V.

References

Bills, B., and F. Nimmo (2005), Rotational dynamics and internal structure of Titan, *Icarus*, *214*, 351–355.

Cammarano, F., V. Lekic, M. Manga, M. Panning, and B. Romanowicz (2006), Long-period seismology on Europa: 1. Physically consistent interior models, *J. Geophys. Res.*, *111*, E12009, doi:10.1029/2006JE002710.

Castillo-Rogez, J., and T. McCord (2010), Ceres' evolution and present state constrained by shape data, *Icarus*, *205*(2), 443–459.
Castillo-Rogez, J. C. (2011), Ceres—Neither a porous nor salty ball, *Icarus*, *215*, 599–602.
Catling, D. C., and M. W. Claire (2005), How Earth's atmosphere evolved to an oxic state: A status report, *Earth Planet. Sci. Lett.*, *237*(1), 1–20.
Chyba, C. F., D. G. Jankowski, and P. D. Nicholson (1989), Tidal evolution in the Neptune-Triton system, *Astron. Astrophys.*, *219*, L23–L26.
Cooper, J., P. Cooper, E. Sittler, S. Sturner, and A. Rymer (2009), Old Faithful model for radiolytic gas-driven cryovolcanism at Enceladus, *Planet. Space Sci.*, *57*(13), 1607–1620.
Cooper, J. F., R. E. Johnson, B. H. Mauk, H. B. Garrett, and N. Gehrels (2001), Energetic ion and electron irradiation of the icy Galilean satellites, *Icarus*, *149*(1), 133–159.
deMartin, B. J., R. A. Sohn, J. P. Canales, and S. E. Humphris (2007), Kinematics and geometry of active detachment faulting beneath the Trans-Atlantic Geotraverse (TAG) hydrothermal field on the Mid-Atlantic Ridge, *Geology*, *35*(8), 711–714.
Farough, A., D. Moore, D. Lockner, and R. Lowell (2016), Evolution of fracture permeability of ultramafic rocks undergoing serpentinization at hydrothermal conditions: An experimental study, *Geochem. Geophys. Geosyst.*, *17*, 44–55, doi:10.1002/2015GC005973.
Flowers, R., S. Bowring, and P. Reiners (2006), Low long-term erosion rates and extreme continental stability documented by ancient (U-Th)/He dates, *Geology*, *34*(11), 925–928.
Früh-Green, G. L., J. A. Connolly, A. Plas, D. S. Kelley, and B. Grobéty (2004), Serpentinization of oceanic peridotites: Implications for geochemical cycles and biological activity, in *The Subseafloor Biosphere at Mid-Ocean Ridges*, edited by W. S. Wilcock et al., pp. 119–136, AGU, Washington, D. C.
Fyfe, W. (1985), Fluids, tectonics and crustal deformation, *Tectonophysics*, *119*(1), 29–36.
Glein, C. R., J. A. Baross, and J. H. Waite (2015), The pH of Enceladus' ocean, *Geochim. Cosmochim. Acta*, *162*, 202–219.
Greenberg, R. (2010), Transport rates of radiolytic substances into Europa's ocean: Implications for the potential origin and maintenance of life, *Astrobiology*, *10*(3), 275–283.
Hand, K., R. Carlson, and C. Chyba (2007), Energy, chemical disequilibrium, and geological constraints on Europa, *Astrobiology*, *7*(6), 1006–1022.
Hand, K., C. Chyba, J. Priscu, R. Carlson, and K. Nealson (2009), *Astrobiology and the Potential for Life on Europa*, 589 pp., Ariz. Univ. Press, Tucson.
Hayes, J. M., and J. R. Waldbauer (2006), The carbon cycle and associated redox processes through time, *Philos. Trans. R. Soc. B*, *361*(1470), 931–950.
Holland, H. D. (2002), Volcanic gases, black smokers, and the great oxidation event, *Geochim. Cosmochim. Acta*, *66*(21), 3811–3826.
Hsu, H.-W., et al. (2015), Ongoing hydrothermal activities within Enceladus, *Nature*, *519*(7542), 207–210.
Hussmann, H., and T. Spohn (2004), Thermal-orbital evolution of Io and Europa, *Icarus*, *171*(2), 391–410.
Hussmann, H., F. Sohl, and T. Spohn (2006), Subsurface oceans and deep interiors of medium-sized outer planet satellites and large trans-neptunian objects, *Icarus*, *185*, 258–273.
Iess, L., et al. (2012), The tides of Titan, *Science*, *337*(6093), 457–459.
Iess, L., et al. (2014), The gravity field and interior structure of Enceladus, *Science*, *344*(6179), 78–80.
Jakosky, B. M., and E. L. Shock (1998), *J. Geophys. Res.*, *103*(E8), 19,359–19,364.
Johnson, H. P., and M. J. Pruis (2003), Fluxes of fluid and heat from the oceanic crustal reservoir, *Earth Planet. Sci. Lett.*, *216*(4), 565–574.
Johnson, R. (2004), The magnetospheric plasma-driven evolution of satellite atmospheres, *Astrophys. J. Lett.*, *609*, L99–L102.
Kattenhorn, S. A., and L. M. Prockter (2014), Evidence for subduction in the ice shell of Europa, *Nat. Geosci.*, *7*(10), 762–767.
Kelemen, P. B., and G. Hirth (2012), Reaction-driven cracking during retrograde metamorphism: Olivine hydration and carbonation, *Earth Planet. Sci. Lett.*, *345*, 81–89.
Khurana, K., M. Kivelson, D. Stevenson, G. Schubert, C. Russell, R. Walker, and C. Polanskey (1998), Induced magnetic fields as evidence for subsurface oceans in Europa and Callisto, *Nature*, *395*(6704), 777–780.
Kivelson, M., K. Khurana, and M. Volwerk (2002), The permanent and inductive magnetic moments of Ganymede, *Icarus*, *157*(2), 507–522.
Lane, N., and W. Martin (2010), The energetics of genome complexity, *Nature*, *467*(7318), 929–934.
Lin, L.-H., G. F. Slater, B. S. Lollar, G. Lacrampe-Couloume, and T. Onstott (2005), The yield and isotopic composition of radiolytic H_2, a potential energy source for the deep subsurface biosphere, *Geochim. Cosmochim. Acta*, *69*(4), 893–903.
Lowell, R. P., and M. DuBose (2005), Hydrothermal systems on Europa, *Geophys. Res. Lett.*, *32*, L05202, doi:10.1029/2005GL022375.
MacDonald, A. H., and W. S. Fyfe (1985), Rate of serpentinization in seafloor environments, *Tectonophysics*, *116*(1–2), 123–135.
Maruyama, S., M. Ikoma, H. Genda, K. Hirose, T. Yokoyama, and M. Santosh (2013), The naked planet Earth: Most essential pre-requisite for the origin and evolution of life, *Geosci. Frontiers*, *4*(2), 141–165.
Mayhew, L., E. Ellison, T. McCollom, T. Trainor, and A. Templeton (2013), Hydrogen generation from low-temperature water-rock reactions, *Nat. Geosci.*, *6*(6), 478–484.
McCaig, A. (1988), Deep fluid circulation in fault zones, *Geology*, *16*(10), 867.
McCord, T. B., and C. Sotin (2005), Ceres: Evolution and current state, *J. Geophys. Res.*, *110*(E5), E05009, doi:10.1029/2004JE002244.
Michalski, J. R., J. Cuadros, P. B. Niles, J. Parnell, A. D. Rogers, and S. P. Wright (2013), Groundwater activity on Mars and implications for a deep biosphere, *Nat. Geosci.*, *6*(2), 133–138.
Neveu, M., S. J. Desch, and J. C. Castillo-Rogez (2015), Core cracking and hydrothermal circulation can profoundly affect Ceres' geophysical evolution, *J. Geophys. Res. Planets*, *120*(2), 123–154, doi:10.1002/2014JE004714.
Nielsen, S. G., M. Rehkämper, D. A. Teagle, D. A. Butterfield, J. C. Alt, and A. N. Halliday (2006), Hydrothermal fluid fluxes calculated from the isotopic mass balance of thallium in the ocean crust, *Earth Planet. Sci. Lett.*, *251*(1), 120–133.
Nimmo, F., and J. Spencer (2014), Powering Triton's recent geological activity by obliquity tides: Implications for Pluto geology, *Icarus*, *246*, 2–10.
O'Hanley, D. (1992), Solution to the volume problem in serpentinization, *Geology*, *20*, 705–708.
Panning, M., V. Lekic, M. Manga, and B. Romanowicz (2006), Long-period seismology on Europa: 2. Predicted seismic response, *J. Geophys. Res.*, E12008, doi:10.1029/2006JE002712.
Pappalardo, R., et al. (2013), Science potential from a Europa lander, *Astrobiology*, *13*(8), 740–773.
Pasek, M. A., and R. Greenberg (2012), Acidification of Europa's subsurface ocean as a consequence of oxidant delivery, *Astrobiology*, *12*(2), 151–159.
Pauer, M., S. Musiol, and D. Breuer (2010), Gravity signals on Europa from silicate shell density variations, *J. Geophys. Res.*, *115*, E12005, doi:10.1029/2010JE003595.
Picard, A., and I. Daniel (2013), Pressure as an environmental parameter for microbial life—A review, *Biophys. Chem.*, *183*, 30–41.
Pittis, A. A., and T. Gabaldón (2016), Late acquisition of mitochondria by a host with chimaeric prokaryotic ancestry, *Nature*, *531*(7592), 101–104.

Postberg, F., S. Kempf, J. Schmidt, N. Brilliantov, A. Beinsen, B. Abel, U. Buck, and R. Srama (2009), Sodium salts in E-ring ice grains from an ocean below the surface of Enceladus, *Nature*, *459*(7250), 1098–1101.
Rhoden, A. R., W. Henning, T. A. Hurford, and D. P. Hamilton (2015), The interior and orbital evolution of charon as preserved in its geologic record, *Icarus*, *246*, 11–20.
Rothschild, L., and R. Mancinelli (2001), Life in extreme environments, *Nature*, *409*(6823), 1092–1101.
Russell, M. J., et al. (2014), The drive to life on wet and icy worlds, *Astrobiology*, *14*(4), 308–343.
Schmidt, B., D. Blankenship, G. Patterson, and P. Schenk (2011), Active formation of chaos terrain over shallow subsurface water on Europa, *Nature*, *479*(7374), 502–505.
Schubert, G., J. Anderson, T. Spohn, and W. McKinnon (2004), Interior composition, structure and dynamics of the Galilean satellites, in *Jupiter: The Planet, Satellites and Magnetosphere*, pp. 281–306, Cambridge Univ. Press, Cambridge, U. K.
Sherwood Lollar, B., K. Voglesonger, L. Lin, G. Lacrampe-Couloume, J. Telling, T. Abrajano, T. Onstott, and L. Pratt (2007), Hydrogeologic controls on episodic H_2 release from Precambrian fractured rocks-Energy for deep subsurface life on Earth and Mars, *Astrobiology*, *7*(6), 971–986.
Sherwood Lollar, B., T. Onstott, G. Lacrampe-Couloume, and C. Ballentine (2014), The contribution of the Precambrian continental lithosphere to global H_2 production, *Nature*, *516*(7531), 379–382.
Sleep, N. (2012), Maintenance of permeable habitable subsurface environments by earthquakes and tidal stresses, *Int. J. Astrobiol.*, *1*(1), 1–12.
Sleep, N., and D. Bird (2007), Niches of the pre-photosynthetic biosphere and geologic preservation of Earth's earliest ecology, *Geobiology*, *5*(2), 101–117.
Sleep, N., A. Meibom, T. Fridriksson, R. Coleman, and D. Bird (2004), H_2-rich fluids from serpentinization: Geochemical and biotic implications, *Proc. Natl. Acad. Sci.*, *101*, 12,818–12,823.
Sotin, C., G. Tobie, J. Wahr, and W. McKinnon (2009), Tides and tidal heating on Europa, in *Europa*, pp. 85–117, Univ. of Ariz. Press, Tucson.
Takir, D., J. P. Emery, H. Y. Mcsween, C. A. Hibbitts, R. N. Clark, N. Pearson, and A. Wang (2013), Nature and degree of aqueous alteration in CM and CI carbonaceous chondrites, *Meteor. Planet. Sci.*, *48*(9), 1618–1637.
Travis, B., J. Palguta, and G. Schubert (2012), A whole-moon thermal history model of Europa: Impact of hydrothermal circulation and salt transport, *Icarus*, *218*, 1006–1019.
Tutolo, B. M., D. F. Mildner, C. V. Gagnon, M. O. Saar, and W. E. Seyfried (2016), Nanoscale constraints on porosity generation and fluid flow during serpentinization, *Geology*, *44*(2), 103–106.
Vance, S., and J. Goodman (2009), *Oceanography of an Ice-Covered Moon, Europa*, edited by R. T. Pappalardo, W. B. McKinnon, and K. K. Khurana, pp. 459–482, Ariz. Univ. Press, Tucson.
Vance, S., J. Harnmeijer, J. Kimura, H. Hussmann, B. deMartin, and J. M. Brown (2007), Hydrothermal systems in small ocean planets, *Astrobiology*, *7*(6), 987–1005.
Vance, S., M. Bouffard, M. Choukroun, and C. Sotin (2014), Ganymede's internal structure including thermodynamics of magnesium sulfate oceans in contact with ice, *Planet. Space Sci.*, *96*, 62–70.
Vance, S., J. H. Roberts, and A. Ganse (2015), Inverse theory for planning gravity investigations of icy moons, in *46th Lunar and Planetary Science Conference*, p. 2751, LPI Contribution No. 1832, Woodlands, Tex.
von Strandmann, P. A. P., E. E. Stüeken, T. Elliott, S. W. Poulton, C. M. Dehler, D. E. Canfield, and D. C. Catling (2015), Selenium isotope evidence for progressive oxidation of the neoproterozoic biosphere, *Nat. Commun.*, *6*, 10157.
Wagner, W., and A. Pruss (2002), The IAPWS formulation 1995 for the thermodynamic properties of ordinary water substance for general and scientific use, *J. Phys. Chem. Ref. Data*, *31*(2), 387–535.
Waite, J. H., et al. (2009), Liquid water on Enceladus from observations of ammonia and ^{40}Ar in the plume, *Nature*, *460*(7254), 487–490.
Zahnle, K., J. L. Alvarellos, A. Dobrovolskis, and P. Hamill (2008), Secondary and sesquinary craters on Europa, *Icarus*, *194*, 670–674.
Zhang, S., et al. (2016), Sufficient oxygen for animal respiration 1,400 million years ago, *Proc. Natl. Acad. Sci.*, *113*, 1731–1736.
Zolotov, M. Y., and J. Kargel (2009), *On the Chemical Composition of Europa's Icy Shell, Ocean, and Underlying Rocks, Europa*, edited by R. T. Pappalardo, W. B. McKinnon, and K. Khurana, pp. 431–458, Univ. of Ariz. Press, Tucson.

Erratum

In the originally published version of this article, graphical artifacts resulting from a software incompatibility issue were found in Figure 1. The replacement to Figure 1 removes graphical artifacts and this version may be considered the authoritative version of record.